# Effect of retained austenite and high temperature Laves phase on the work hardening of an experimental maraging steel

S. W. Ooi[a], P. Hill[b], M. Rawson[b], H. K. D. H. Bhadeshia[a]

[a]*Department of Materials Science and Metallurgy, University of Cambridge, Cambridge, U.K.*
[b]*Rolls-Royce plc, Derby, UK*

## Abstract

Maraging steels including the experimental alloy studied here show atypical stress–strain behaviour during tensile testing. In particular, there is a gradual decrease in the ability of the sample to support a stress following a small fraction of the total plastic strain to failure. It is demonstrated here that this phenomenon is not associated with the early onset of a necking instability, and that a large amount of the plastic strain beyond the peak stress is uniform. Investigations of microstructure and retained austenite content reveal that the intrinsic microstructure of maraging steels has a poor ability to work harden. The work hardening capacity can, as expected, be improved by introducing retained austenite, but there is an associated reduction in strength. Experiments have been designed to control the retained austenite content in such a way that clear comparisons can be made and conclusions reached on both the role of the austenite and of Laves phase generated at different temperatures.

*Keywords:* retained austenite, Laves phase, maraging steel

*Email address:* `swo23@cam.ac.uk` (S. W. Ooi)

## 1. Introduction

Maraging steels typically have a very low carbon concentration so that after austenitisation, quenching results in a microstructure which is predominantly soft–martensite, which is then hardened by the precipitation of intermetallic compounds. Some austenite may be retained on quenching, but enriched austenite can grow by reversion if the hardening temperature is too high. Maraging steels are well-known for their outstanding combination of strength, fracture toughness and machinability in the solution annealed condition, minimum distortion during subsequent ageing; depending on the chemical composition, the steel can also be stainless. As a consequence, maraging steels have many applications, for example in the manufacture of crankshafts, gears, tools, rocket and missile casings [1–5].

Many earlier studies of maraging steels have focused on the precipitation behaviour and the effect of austenite reversion during the maraging heat treatment [6–13]; investigations of the effect of the solution treatment condition have focused on maintaining a small austenite grain size [14–17]. The purpose of the present work was to establish in a newly designed high-chromium and low-nickel maraging steel, the effect of retained austenite and high temperature Laves phase formation on the work hardening ability. This is because the stress-strain curve exhibits untypical behaviour where the deformation following the peak stress continues over a large range of plastic strain at gently decreasing stress, prior to final failure. This characteristic is irrespective of whether the stress and strain are plotted as true or engineering values. The understanding of this behaviour is limited [18–22].

## 2. Experimental procedure

The alloy was produced in a vacuum–induction furnace and the composition is shown in Table 1, and cast into a $150 \times 150 \times 410$ mm ingot. After removal of the shrinkage cavity, the remaining material was heated to $1200\,^\circ$C and then forged into a $50 \times 50$ mm cross-section blank. The blank was homogenised at $1200\,^\circ$C for 48 h, furnace cooled, reheated to $1200\,^\circ$C before being hot rolled to 19 mm diameter rod. The martensite-start temperature

2

($M_S$) was measured using a precision dilatometer (Thermecmaster-Z) and the data interpreted using the offset method described elsewhere [23]. The measured martensite-start temperature is also shown in Table 1.

Bars about 80 mm long were cut from the hot-rolled samples. Solution heat–treatments were performed in a box furnace with the temperature range of 725-900 °C for 1 to 30 h, followed by air cooling to room temperature and immersion in liquid nitrogen for 2 h. The subsequent ageing treatment was carried out at 450 °C for 25 h. At the end of the ageing time the sample was air cooled to room temperature.

All tensile test pieces were extracted parallel to the rolling direction from the heat-treated bars and were machined in accordance to British standard (BS EN10002-1-5:2001) to cylindrical tensile test piece with 5 mm diameter and 25 mm gauge length. The specimen is designed to have two collars for extensometer attachment. X-ray analysis was carried out to quantify the volume percentage of retained austenite ($\gamma$) on the colloidal silica polished samples. Metallographic observations were made on the samples etched with Fry's reagent using the JEOL 5800LV scanning electron microscope (SEM). Thin foils for transmission electron microscopy (TEM) were prepared using a twin-jet electro-polisher, with the electrolytic solution consisting of 5 vol% perchloric acid, 25 vol% glycerol and 70 vol% ethanol. The temperature of the solution during thinning was maintained at 10 °C. TEM investigations were conducted on FEI Tecnai 20 electron microscope. Energy-filtered transmission electron microscopy (EFTEM) couple with the jump ratio technique was used to produce qualitative chemical concentration maps of Ni.

## 3. Work hardening and plastic instability of maraging steel

As mentioned in the introduction, maraging steels in general have a low work-hardening ability. The engineering stress-strain curve of the maraging steel has a peak stress at relatively small plastic strains followed by continued decrease of stress, leading to a low tensile to yield-strength ratio [18–22]. However, the observed total elongation is normally large (about 10%). A low tensile to yield strength ratio indicates that the tolerance to plastic overload

is small as the work hardening after yield is minimal. Such a characteristic may become a problem in a safe design against sudden overload, as in this case, it may be necessary to sustain a lot of plastic deformation prior to fracture [24, 25].

An experiment was conducted in which the tensile test was video recorded in order to clarify the mechanism of the softening following the achievement of peak strength. Fig. 1 shows the evolution of the specimen dimensions and the corresponding tensile stress–strain curve of the solution treated (900 °C for 1 h) sample which was then cooled to $-196$ °C for 2 h (henceforth referred to as a cryogenic treatment). Fig. 2 shows similar data for the sample which in addition is aged at 450 °C for 25 h. Both stress–strain curves shown in Figs. 1 and 2 illustrate that the softening of the steel is not caused by plastic instability associated with necking as typical in most steels. Instead, a uniform strain is observed during stages (i) to (iii) of deformation. The true-stress versus true strain curves plotted in Fig. 3 confirm the complete absence of work hardening after the maximum stress is reached at an early stage in the tests.

## 4. Effect of austenitisation condition

Engineering and true tensile curves obtained from samples in the solution and cryogenically treated conditions, and in the aged condition are shown in Fig. 4. The true stress-strain curves in this case are plotted using extensometer data assuming constant volume change. The limiting strain is chosen as 0.1 and 0.08 for solution and aged samples respectively as uniform strain is observed on the tensile samples (Fig. 1 and 2) until these strains. Table 2 lists the heat treatment details, underlining the mechanical properties and measured retained austenite ($\gamma$) content prior to tensile testing.

The selection of the two different solution temperatures was to assess the role of Laves phase since its quantity is a function of temperature as shown in Fig. 5. Austenitisation at low temperature 725 °C will lead to Laves phases formation in austenite, while solution treatment at 900 °C should

leave a single phase austenite. For 725 °C, two different heat treatment times were chosen, the shorter of which would lead to austenite retention (Table 2), while longer austenitisation time eliminates retained austenite, as described later. Thermal grooving was used to reveal the austenite grains for the samples heat–treated at 725 °C for 1 h and 900 °C for 1 h, found to be 23±4 µm and 30±6 µm respectively. Fig. 6 shows typical microstructures as a function of heat–treatment.

A fully martensitic structure without Laves phase is obtained in the sample heat–treated at 900 °C for 1 h. A significant change in morphology is observed in the sample heat–treated at 725 °C for 1 h, where alternating light and dark plate are revealed. The austenite ($\gamma$), which is preferentially etched by Fry's reagent, is shown as dark, while the light regions are martensite. Substantial Laves precipitates (light colour) are observed when solution treatment were performed at 725 °C for 30 h. No noticeable change in microstructure is observed after the ageing treatment.

In the solution+cryogenic treated condition, the highest ultimate tensile strength ($\sigma_m$) is obtained when austenitisation is performed at 725 °C for 1 h and the lowest for 900 °C. Intermediate strength is obtained following 725 °C for 30 h. In the aged condition, austenitisation at 725 °C for 30 h and 900 °C for 1 h led to comparable proof and ultimate strengths, but both values were significantly smaller for austenitisation at 725 °C for 1 h.

About 18 vol% of austenite was retained after austenitisation at 725 °C for 1 h followed by a cryogenic treatment with none detected following heat–treatment at 725 °C for 30 h and 900 °C for 1 h. Table 2 also shows that the ageing treatment also increases the amount of austenite because additional quantities are generated due to reversion. Some 3 to 5 vol% of reverted austenite can form during maraging, even when the austenite is absent prior to ageing. On the other hand, the presence of retained austenite before ageing accelerates the reversion (18 vol% to 26 vol%) as observed in samples austenitized at 725 °C for 1 h. Clearly, extant austenite can simply grow during ageing.

The presence of retained austenite in the solution+cryogenic treated samples increases the work hardening through transformation induced plas-

ticity (TRIP) effect as indicated by the higher tensile to yield strength ratio (table 2) and the increase in tensile strength. However, in the stronger aged condition, the retained austenite results in a reduction of strength. This is because during ageing the martensitic matrix is strengthened by precipitation of intermetallic compounds, while the austenite is not. Even though the austenite is expected to transform into martensite during straining, the martensite formed is not as strong as the maraged martensite. Similary, no significant work hardening is observed due to the TRIP effect.

### 4.1. Effect of high temperature Laves phase

Laves phase generated during heat treatment at $725\,^{\circ}\mathrm{C}$ for $30\,\mathrm{h}$ (Fig. 6e) with no retained austenice present (Table 2), strengthens and introduces a small increase in work hardening compared with when Laves phase is absent ($900\,^{\circ}\mathrm{C}$ for $1\,\mathrm{h}$). In the aged condition, however, this high temperature Laves phase has no significant effect on the work hardening behaviour. Notice that the elongation decreased in both the solution treated and aged conditions when low austenitisation temperature with long heat–treatment time was used; this is caused by the coarse precipitates of Laves phase as revealed on the fracture surface (Fig. 7). Voids also nucleate from large TiN precipitates, which are the inclusions in this alloy. The precipitation of Laves phase during austenitisation will lead to a smaller increment in the strength during aging due to less Laves phase expected to form during ageing.

## 5. Austenite formation and retention

### 5.1. Effect of heating rate

The thermal histories of the steel bars ($19\,\mathrm{mm}$ diameter and $80\,\mathrm{mm}$ long), subjected to austenitisation in a box furnace were recorded as shown in Fig. 9. It is shown that the heating rate experienced by the samples are different when the temperature of the box furnace is varied.

The influences of heating rate during austenitisation was investigated using dilatometry, (Fig. 8). The measured austenite transformation temperatures using offset method ($Ac_1$ and $Ac_3$) were also plotted. A slower heating

6

rate, leads to a larger temperature range ($\Delta T = Ac_3 - Ac_1$) over which austenitisation occurs; this is expected since the superheating to which the steel is exposed is smaller at slow heating rates. This phenomenon was also observed in other types of maraging steel [26]. There are, however, contradictory results reported with $\Delta T$ increasing with the heating rate [27]; this could be because the initial microstructure in these cases consisted of ferrite and pearlite. The presence of cementite which readily initiates austenite, makes the $Ac_1$ temperature insensitive to the heating rate as observed by Oliveira et al. [27], unlike the case for the present alloy as illustrated in Fig. 8b.

*5.2. Austenite reversion*

It is suspected that the exceptionally large quantity of retained austenite observed in the sample subjected to the low austenitisation temperature (725 °C for 1 h) is due to an uneven distribution of nickel, where local enrichment of nickel depresses the martensite-start temperature ($M_S$), causing the retention of austenite. Fig. 10 shows that the maximum solubility of the nickel increase as the temperature is reduced. If the heating rate is slow enough to enable diffusion to happen, then there will be a significant driving force for nickel to partition from martensite into austenite.

In order to verify the stability of the austenite formed and the possibility of nickel partitioning during reheating, an interrupted heat–treatment was performed (Fig. 9), where 31 vol% of austenite is found to be retained in the sample. This experiment proves that the partitioning of nickel into reverted austenite is most likely in the early stages of the heating, thus explaining the difference in retained austenite content for the two samples treated at 725°C, for 1 h and 30 h respectively. The longer time period should reduce the segregated nickel and hence result in a smaller fraction of retained austenite on quenching, consistent with the data presented in Table 2.

As indicated in the dilatometer experiments (Fig. 8a), a slow reheating rate ($0.05 \,°\mathrm{C}\,\mathrm{s}^{-1}$) seems to promote two stages in the transformation into austenite. This phenomenon has been reported in high nickel maraging steels [26, 28, 29]. Kappor [26] claimed that the first stage of austenite reversion

occurs through the long-range diffusion process while the second is by shear transformation. However, the evidence is weak for a displacive mechanism at the higher temperature, and it is more likely that the two–stages are associated with the changing nickel solubility in austenite in contact with martensite as the temperature is increased (Fig. 10).

*5.3. TEM investigation of nickel partitioning*

Transmission electron micrographs of the specimen heat–treated at $725\,^\circ$C for 1 h followed by cryogenic treatment are shown in Fig. 11a with the associated qualitative chemical concentration maps of Ni (Fig. 11b). The brighter areas observed in Fig. 11b is corresponding to higher nickel contents. Fig. 12 shows a bigger area which including the region shown in Fig. 11. It is clearly shown that the retention of austenite is caused by nickel segregation and the heterogeneous nickel distribution, which is caused by the partitioning of nickel during austenite reversion during reheating to $725\,^\circ$C. Figs. 11a and 12 also show that the Laves phase (appeared in reverse contrast) that present in the sample has limited solubility of nickel.

## 6. Discussion and Conclusions

Having proven using *in situ* observations that the tensile test samples deform with uniform plastic strain even after a maximum in the peak stress is reached, with necking occurring at strains well beyond that associated with the maximum stress, it remains to explain in detail the observations summarised in Fig. 4. It is evident that in the sample heat treated at 725°C, 1 h containing some 18% of retained austenite, the plastic strain prior to the point where $\sigma_m$ is reached is large. This can reasonably be attributed to the deformation-induced transformation of retained austenite prolonging the ability of the material to work harden. The relative gradients of the curves beyond $\sigma_m$ as illustrated in Fig. 4b is consistent with this interpretation since the 725°C, 1 h shows more gentle decline in stress beyond $\sigma_m$. However, in the aged condition, the presence of some 26% of retained austenite reduces the maximum achievable strength.

The presence of high temperature Laves phase has a small effect on increasing the work hardening ability prior to the ageing treatment, but is less significant compared to retained austenite. Due to its large size, the Laves phase would act as a void nucleation site, reducing the ductility of the steel in both solution and aged condition.

The absence of Laves phase during austenitisation at 900°C explains why the strength is lower than following the 725°C austenitisation (Fig. 4a), but the deficit is recovered following the ageing heat treatment which also leads to the formation of finer Laves precipitates. The following conclusions may be reached from these studies:

1. Atypical stress–strain curves are observed for the steel studied, and indeed for maraging steels in general, where the peak stress does not correspond to the onset of necking. Instead, there is significant uniform plasticity beyond the peak value, but with negligible work hardening.

2. The presence of retained austenite can enhance the work hardening ability. The austenite can be introduced into the structure by controlling the austenitisation conditions. In particular, austenite that forms in the early stages of heating is likely to be rich in nickel when the heating rate is sufficiently small.

3. The presence of retained austenite in the maraged condition leads to a reduction in the strength, but nevertheless an increased work hardening contribution to the stress–strain behaviour.

**Acknowledgements**

9

[1] G. Avadhani, Journal of Materials Engineering and Performance 12 (2003) 609–622.

[2] K. Rajan, K. Narasimhan, Journal of Materials Engineering and Performance 11 (2002) 444–449.

[3] G. Agas'yants, G. Semibratov, G. Kodjaspirov, Metal Science and Heat Treatment 49 (2007) 29–31.

[4] Y. Wang, Surface and Coatings Technology 94-95 (1997) 60–63.

[5] P. Würzinger, R. Rabitsch, W. Meyer, Journal of Materials Science 39 (2004) 7295–7302.

[6] A. F. Edneral, O. P. Zhukov, M. D. Perkas, Metal Science and Heat Treatment 13 (1971) 276–280.

[7] C. A. Pampillo, H. W. Paxton, Metallurgical Transactions 3 (1972) 2895–2903.

[8] A. F. Edneral, O. P. Zhukov, M. D. Perkas, Metal Science and Heat Treatment 16 (1974) 840–843.

[9] A. Yukiteru, Transactions of the Japan Institute of Metals 28 (1987) 281–290.

[10] V. K. Vasudevan, S. J. Kim, C. Wayman, Metallurgical Transactions. A, Physical Metallurgy and Materials Science 21 A (1990) 2655–2668.

[11] Y. B. Guo, M. E. Barkey, International Journal of Fatigue 26 (2003) 605–613.

[12] Y. He, K. Yang, W. Sha, D. J. Cleland, Metallurgical and Materials Transactions A: Physical Metallurgy and Materials Science 35 (2004) 2747–2755.

[13] S. D. Erlach, H. Leitner, M. Bischof, H. Clemens, F. Danoix, D. Lemarc-hand, I. Siller, Materials Science and Engineering A 429 (2006) 96–106.

[14] Y. He, K. Yang, W. S. Qu, F. Y. Kong, G. Y. Su, Materials Science and Technology 19 (2003) 117–124.

[15] H. J. Rack, Materials Science and Engineering 34 (1978) 263–270.

[16] H. J. Rack, Scripta Metallurgica 13 (1979) 577–582.

[17] G. Saul, J. A. Roberson, A. M. Adair, Metallurgical Transactions 1 (1970) 383–387.

[18] K. Nakashima, Y. Fujimura, T. Tsuchiyama, S. Takaki, in: Materials Science Forum, volume 539-543, pp. 4783–4788.

[19] K. Nakashima, Y. Fujimura, T. Tsuchiyama, S. Takaki, in: Key Engineering Materials, volume 345–346 I, pp. 189–192.

[20] V. Seetharaman, R. Krishnan, Journal of Materials Science 16 (1981) 523–530.

[21] H. Liu, L. Zhou, Transactions of the China Welding Institution 28 (2007) 101–104.

[22] C. Mukhopadhyay, K. Rajkumar, T. Jayakumar, B. Raj, Journal of Materials Science 45 (2010) 1371–1384.

[23] H.-S. Yang, H. K. D. H. Bhadeshia, Materials Science and Technology 23 (2007) 556–560.

[24] A. Elnashai, in: Building in Steel, Insitute of Metals, London, U.K., 1991, pp. 25–32.

[25] M. Toyoda, Welding Journal 74 (1995) 31–42.

[26] R. Kapoor, I. Batra, Materials Science and Engineering A 371 (2004) 324–334.

[27] F. L. G. Oliveira, M. S. Andrade, A. B. Cota, Materials Characterization 58 (2007) 256–261.

[28] C. Servant, P. Lacombe, Journal of Materials Science 12 (1977) 1807–1826.

[29] A. Goldberg, D. G. O'Connor, Nature 14 (1967) 99.

**List of Figures**

Figure 1: Evolution of tensile specimen shape and corresponding engineering stress-strain curve during tensile testing for solution treated specimen. The complete heat–treatment given to the sample prior to testing is $900\,^{\circ}\text{C}$ for $1\,\text{h}$, $-196\,^{\circ}\text{C}$ for $2\,\text{h}$.

Figure 2: Evolution of tensile specimen shape and corresponding engineering stress-strain curve during tensile testing for aged specimen. The complete heat–treatment given to the sample prior to testing is 900 °C for 1 h, -196 °C for 2 h and 450 °C for 25 h.

Figure 3: True stress-strain curve for solution treated and aged specimen plotted using the measured cross section of the specimen from the recorded images. Labels are as in Fig. 1 and 2.
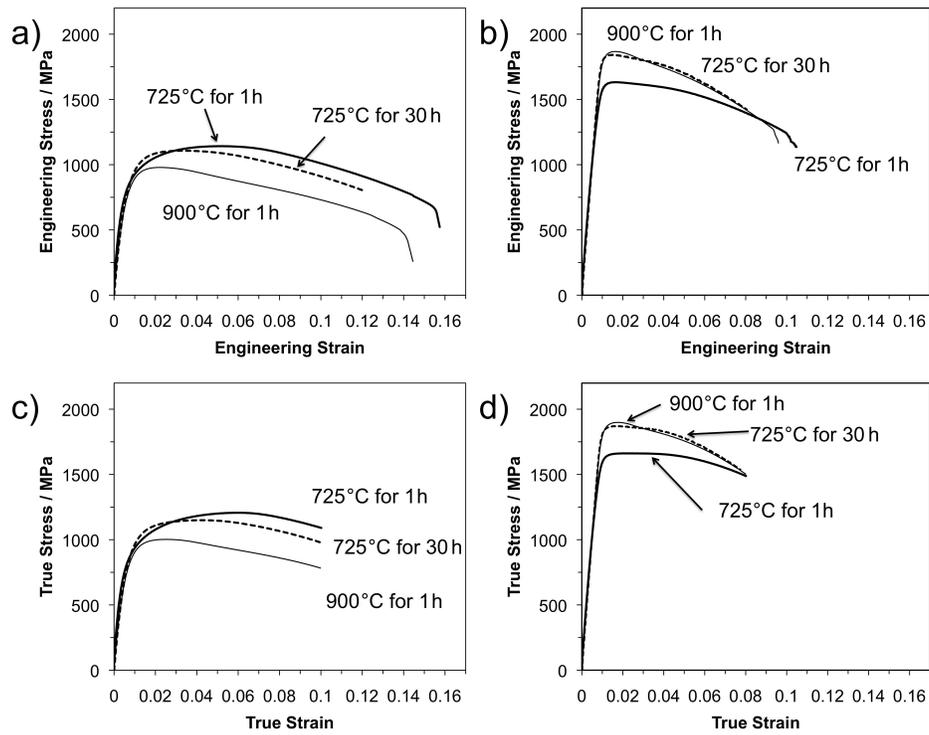
Figure 4: Effect of different solution treatments on the shape of the tensile curve. Engineering stress-strain curve: (a) After solution and cryogenic treatment. (b) As in (a) but following an addition of ageing treatment. True stress-strain curve plotted using extensometer data: (c) After solution and cryogenic treatment. (d) As in (a) but following an addition of ageing treatment.

18
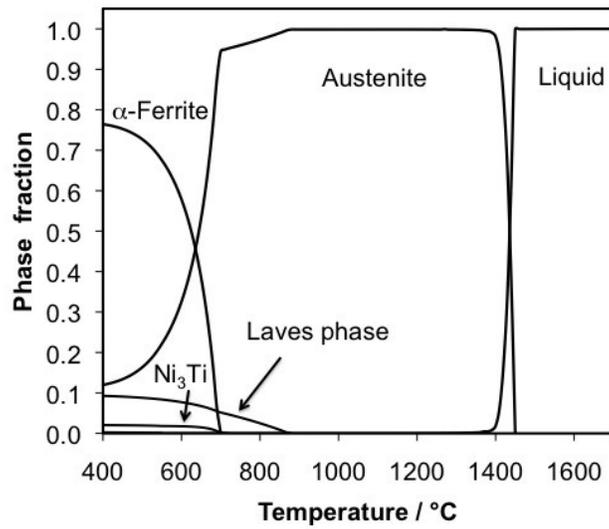
Figure 5: Equilibrium phase fractions of the investigated alloy estimated using MTDATA.
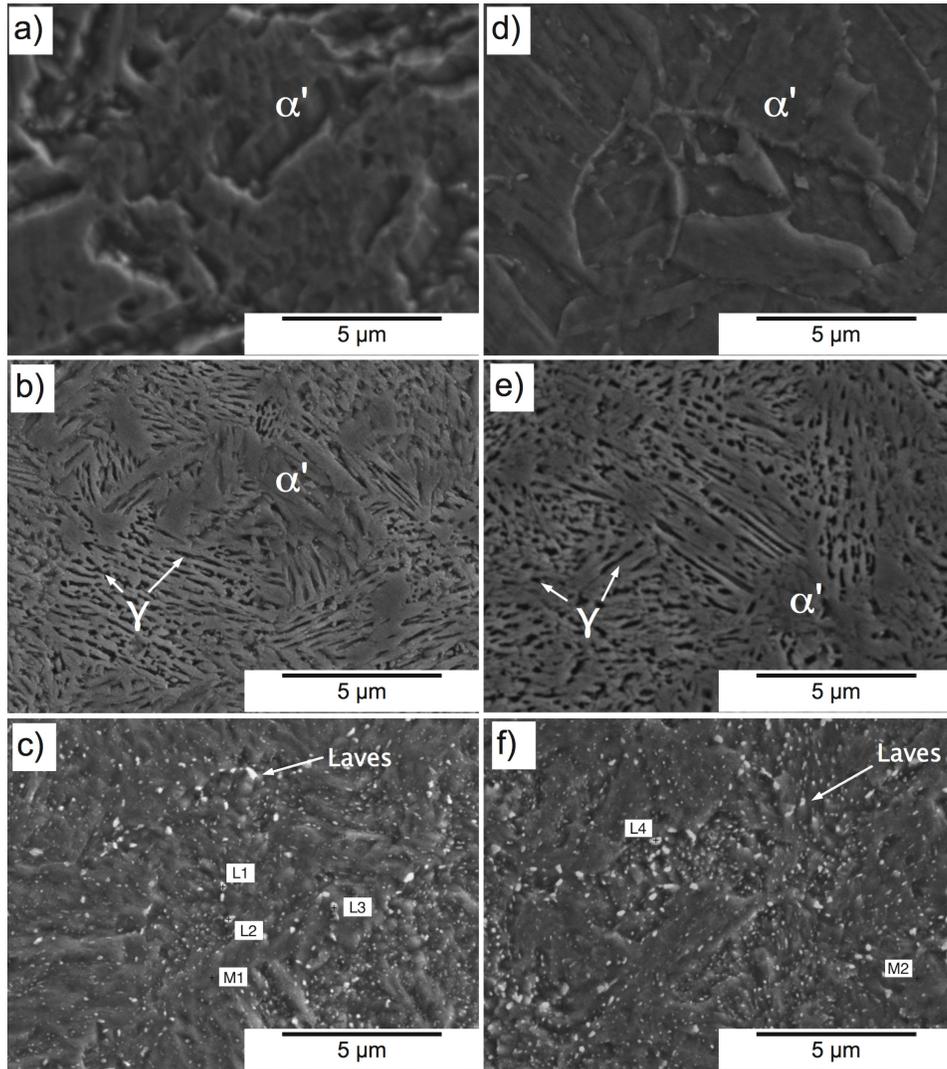
Figure 6: Micrographs of the investigated alloy undergo different heat–treatments. (a) Heat treatment A. (b) Heat treatment B. (c) Heat treatment C. (d) Heat treatment D. (e) Heat treatment E. (f) Heat treatment F. The measured chemical composition of the matrix (M1–2) and precipitate (L1–6) shown is listed in Table 3.
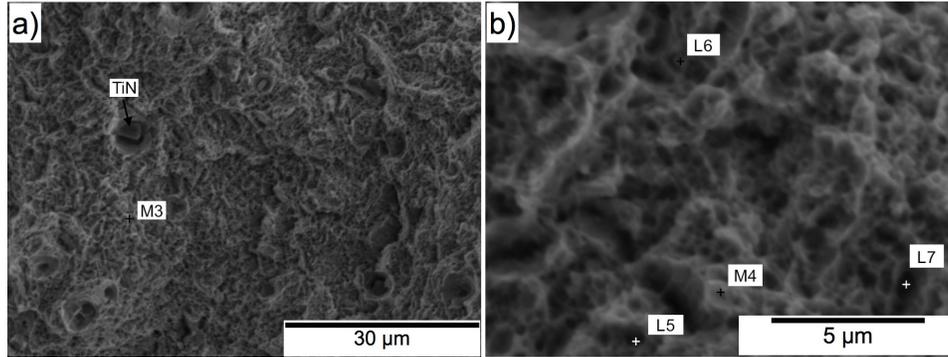
Figure 7: Fracture surface of solution treated sample with austenitisation condition of 725 °C for 30 h (a) large void nucleated on TiN precipitate, while (b) micro void caused by Laves phase. The measured chemical composition shown is listed in Table 4.



(a)

(b)
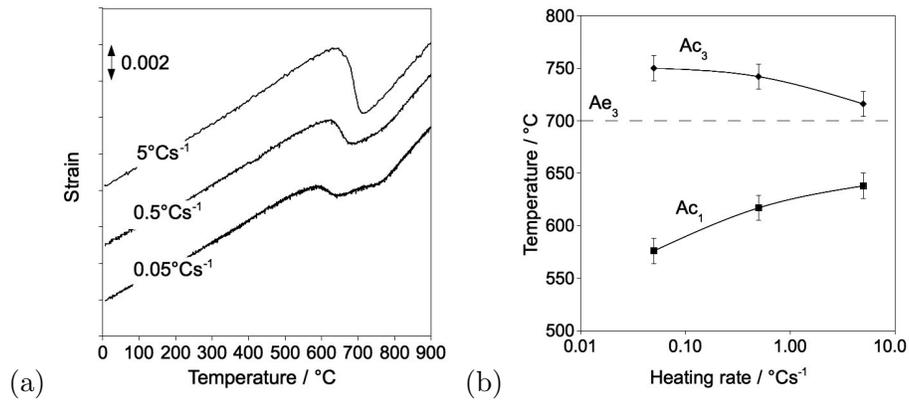
Figure 8: (a) Effect of heating rate on the dilatation curve in the investigated alloy. (b) Effect of heating rate on transformation temperature in the investigated alloy. Also indicate in the figure was $Ae_3$ temperature calculated from MTDATA.
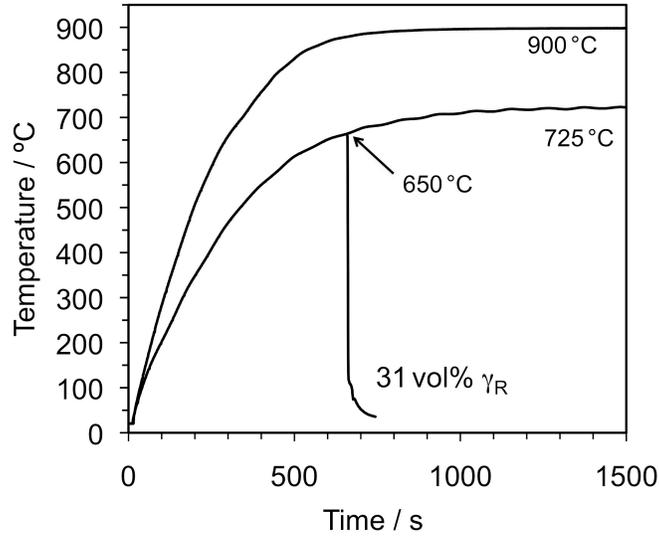
Figure 9: Thermal history of a steel piece (19 mm diameter and 80 mm long) during reheating to austenitisation temperature in a box furnace. An interrupted experiment (up to 650 °C) were performed with the temperature of the box furnace is set at 725 °C was also performed.
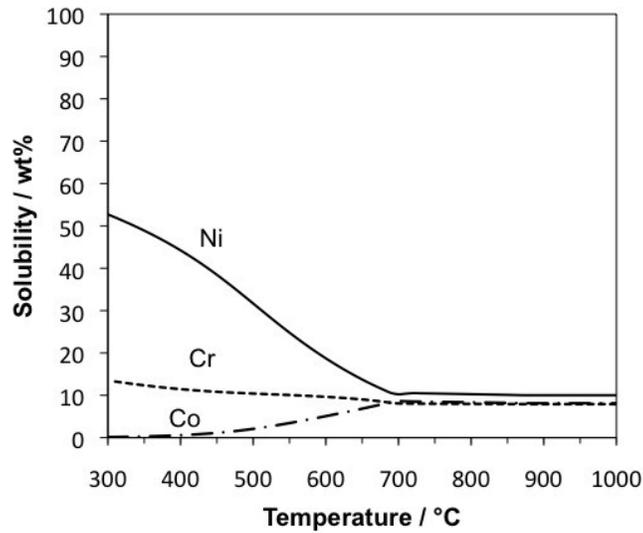


Figure 10: Solubility of different elements in austenite in equilibrium with ferrite, Laves phase and Ni$_3$Ti for the investigated alloy calculated with MTDATA.

22
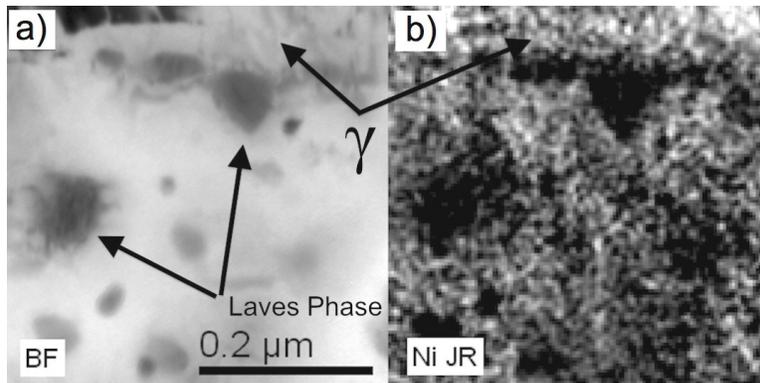
Figure 11: (a) Bright field image and associated qualitative chemical concentration maps of Ni (b). Brighter areas correspond to higher nickel contents.
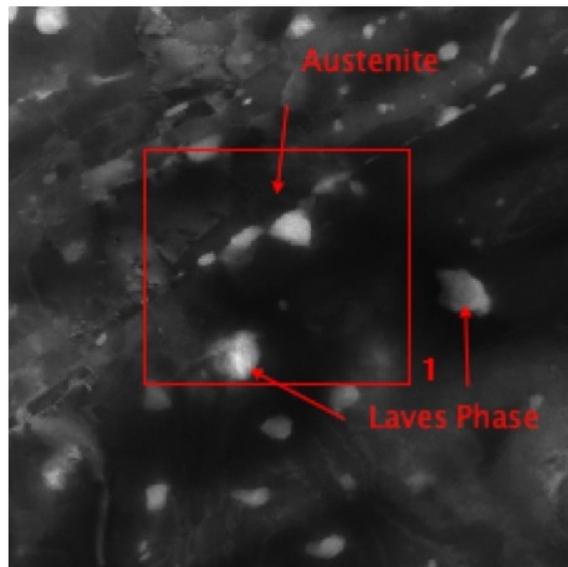


Figure 12: Z-contrast or Annular dark-field (ADF) image with the area where the bright field image and associated qualitative chemical concentration maps of Ni is shown in Fig. 11. Note that the light region in this image is corresponding to the high concentration of heavy elements, molybdenum and tungsten in this case.

## List of Tables

Table 1: The chemical composition of the experimental maraging steel (in wt%). The $M_S$ temperature was measured at a cooling rate of $30\,°\mathrm{C\,s}^{-1}$.

| C | N | Ni | Cr | Co | Mo | W | Ti | Al | $M_S$ / °C |
|---|---|----|----|----|----|---|----|----|----|
| 0.013 | 0.013 | 10.02 | 7.93 | 8.14 | 2.79 | 2.29 | 0.49 | 0.2 | 97±12 |

Table 2: Effect of heat–treatments on the measured retained austenite austenite content and mechanical properties. The term 'cryogenic' refers to -196 °C for 2 h, and 'aged' to a heat treatment at 450 °C for 25 h. $\sigma_P$ is the 0.2% proof strength, $\sigma_m$ the ultimate tensile strength and $\delta$ the elongation.

| Label | Heat–treatment | $\gamma$ vol% | $\sigma_P$ MPa | $\sigma_m$ MPa | $\sigma_m/\sigma_P$ | $\delta$ % |
|-------|----------------|------|------|------|------|------|
| A | 900 °C 1 h, cryogenic | 0 | 817 | 979 | 1.20 | 14.6 |
| B | 725 °C 1 h, cryogenic | 18±1 | 834 | 1142 | 1.37 | 15.7 |
| C | 725 °C 30 h, cryogenic | 0 | 839 | 1107 | 1.32 | 12.0 |
| D | 900 °C 1 h, cryogenic, aged | 5±1 | 1817 | 1867 | 1.03 | 9.6 |
| E | 725 °C 1 h, cryogenic, aged | 26±1 | 1559 | 1632 | 1.05 | 10.5 |
| F | 725 °C for 30 h, cryogenic, aged | 3±1 | 1788 | 1842 | 1.03 | 8.0 |

Table 3: Corresponding measured chemical composition of precipitate and matrix in Fig. 6.

| Elements / wt% | Ti | Cr | Fe | Co | Ni | Mo | W |
|---|---|---|---|---|---|---|---|
| Precipitates (L1) | 0.82±0.4 | 7.7±0.7 | 49.0±1.7 | 8.0±1.3 | 7.6±1.4 | 13.1±1.2 | 13.3±1.1 |
| Precipitates (L2) | 0.29±0.4 | 8.5±0.7 | 55.7±1.8 | 6.7±1.4 | 8.8±1.3 | 10.0±1.1 | 9.8±1.0 |
| Precipitates (L3) | 0.56±0.4 | 8.3±0.8 | 57.1±1.8 | 5.7±1.4 | 8.4±1.4 | 10.2±1.1 | 9.7±1.0 |
| Precipitates (L4) | 0.62±0.4 | 7.1±0.7 | 53.5±1.6 | 8.9±1.2 | 7.6±1.0 | 11.2±1.0 | 11.1±1.0 |
| Matrix (M1) | 0.50±0.4 | 7.7±0.7 | 64.5±1.8 | 10.2±1.3 | 10.2±1.4 | 3.9±0.9 | 3.1±0.8 |
| Matrix (M2) | 0.35±0.4 | 9.3±0.7 | 65.3±1.7 | 8.1±1.3 | 10.2±1.3 | 3.1±0.8 | 3.6±0.8 |

Table 4: Chemical compositions of regions identified in Fig. 7.

| Elements / wt% | Al | Ti | Cr | Fe | Co | Ni | Mo | W |
|---|---|---|---|---|---|---|---|---|
| Precipitates (TiN) | 0.0±0.0 | 70.2±0.4 | 3.5±0.2 | 20.8±0.3 | 3.0±0.3 | 1.8±0.2 | 0.7±0.1 | 0.0±0.0 |
| Precipitates (L5) | 0.3±0.1 | 0.4±0.1 | 8.5±0.2 | 64.4±0.4 | 8.3±0.3 | 9.6±0.3 | 4.5±0.2 | 4.2±0.2 |
| Precipitates (L6) | 0.2±0.1 | 0.4±0.1 | 8.7±0.2 | 64.6±0.4 | 8.2±0.3 | 10.1±0.3 | 4.1±0.2 | 3.7±0.2 |
| Precipitates (L7) | 0.3±0.1 | 0.4±0.1 | 8.5±0.2 | 65.1±0.4 | 8.6±0.3 | 9.2±0.3 | 4.1±0.2 | 3.8±0.2 |
| Matrix (M3) | 0.2±0.1 | 0.4±0.1 | 8.4±0.1 | 67.7±0.2 | 8.9±0.2 | 9.1±0.2 | 2.9±0.1 | 2.4±0.1 |
| Matrix (M4) | 0.3±0.1 | 0.4±0.1 | 8.8±0.2 | 66.8±0.4 | 8.6±0.3 | 9.6±0.3 | 3.0±0.2 | 2.5±0.2 |